Research Article

Received: 1 December 2021 Revised: 25 April 2022 Accepted article published: 3 May 2022 Published online in Wiley Online Library: 30 May 2022

(wileyonlinelibrary.com) DOI 10.1002/jctb.7105

Bioprocess characterization of virus-like particle production with the insect cell baculovirus expression system at nanoparticle level

Eduard Puente-Massaguer,[a*†] Irene González-Domínguez,[a] Florian Strobl,[b,c] Reingard Grabherr,[c] Gerald Striedner,[c] Martí Lecina[d] and Francesc Gòdia[a]

Abstract

Background. Virus-like particles (VLPs) are a multivalent platform showing great promise for the development of vaccines, gene therapy, diagnostic, and drug delivery approaches. Particularly, HIV-1 Gag VLPs provide a robust and flexible scaffold for the presentation of a variety of antigens. The insect cell baculovirus expression vector system (BEVS) is nowadays one of the reference systems to produce these complex nanoparticles, but information about VLP quality, quantity, stability, as well as cell performance is scarce, especially at bioreactor scale. Results. VLPs produced in the reference High Five and Sf9 insect cell lines share similar physicochemical properties, with VLPs produced in Sf9 cells showing lower levels of double stranded DNA and protein contaminants, and a higher degree of VLP assembly. Besides VLPs, other nanoparticle populations are divergently encountered in each cell line. Hi5 supernatants contain a higher load of extracellular vesicles, while Sf9 supernatants exhibit higher concentrations of baculovirus particles. Similar titers are achieved when comparing Gag to Gag-eGFP VLP production, with the size of most of the nanoparticles produced comprised at the 150–250 nm range. Eventually, Gag VLP production in a 2 L stirred tank bioreactor is successfully demonstrated, validating bioprocess transference to the final product candidate. Conclusions. This work provides two potentially valuable strategies for the production of HIV-1 Gag VLPs and a detailed analysis of the different nanoparticle populations produced.

Supporting information may be found in the online version of this article.

Keywords: insect cells; virus-like particle; HIV-1; baculovirus; bioreactor; super-resolution fluorescence microscopy

INTRODUCTION

The baculovirus expression vector system (BEVS) has become one of the gold standards for recombinant protein production. Since its development in the early 1980s, the BEVS has experienced an unprecedented evolution[1] and is nowadays considered a robust technology to produce high levels of recombinant proteins in short times.[2] A variety of products have been produced with this system, ranging from very simple recombinant proteins[3] to more complex products including adeno-associated virus vectors[4] and virus-like particles (VLPs).[5]

VLPs are self-assembling nanoparticles made of one or several structural proteins of the native virus. These nanoparticles closely resemble the original virus structure but, unlike wild-type viruses, are devoid of viral genetic material.[6] The main field of application of VLPs is in vaccine development since they have shown to elicit robust and broad immune responses that are capable of engaging B and T cells.[7] Currently, several prophylactic VLP-based vaccines are commercially available for Hepatitis B, E, human papillomavirus, and malaria.[8] The versatility of VLPs is not restricted to vaccines, with successful results reported in gene therapy,[9,10] drug delivery,[11,12] theragnostic,[13] and *in vitro*

* *Correspondence to: E Puente-Massaguer, Departament d'Enginyeria Química, Biològica i Ambiental, Universitat Autònoma de Barcelona, Barcelona, Spain. E-mail: eduard.puente-massaguer@mssm.edu*

† *Present address: Department of Microbiology, Icahn School of Medicine at Mount Sinai, 10029, New York, USA*

a *Departament d'Enginyeria Química, Biològica i Ambiental, Universitat Autònoma de Barcelona, Barcelona, Spain*

b *Austrian Centre of Industrial Biotechnology (acib GmbH), Vienna, Austria*

c *Department of Biotechnology, University of Natural Resources and Life Sciences, Vienna, Austria*

d *IQS School of Engineering, Universitat Ramón Llull, Barcelona, Spain*

diagnostic approaches.[14] Among the different VLP candidates available, Gag-based VLPs have shown great promise in a variety of applications by providing a stable scaffold for membrane protein presentation against infectious diseases,[15] as an active cancer immunotherapy,[16] and for protein delivery.[17]

The production of enveloped VLPs is generally accomplished in mammalian or insect cell lines[18] and through different expression systems,[19,20] with the insect cell/BEVS being generally unrivalled.[21] Sf9, a clonal isolate derived from the parental *Spodoptera frugiperda* cell line IPLB-Sf-21-AE, and High Five (Hi5, BTI-TN-5B1-4) insect cells are generally the choice to produce recombinant products with this system. Sf9 cells are known to achieve higher baculovirus (BV) titers, whereas Hi5 cells are typically used for recombinant protein production. Advances in the field of nanoparticle characterization and quantification have opened the opportunity to characterize the production of complex products at nanoparticle level. Moreover, progress made in the field of cell culture media development in recent years has put the basis for the intensification and standardization of recombinant protein production with the BEVS. In this sense, we recently assessed and optimized the production of Gag-eGFP VLPs with the BEVS in both insect cell lines cultured in shake flasks.[22,23] Bioprocess validation using the final candidate product, its stability, and the transference to larger volumes are key aspects for the success of any given bioprocess. It has been a long time since the last attempts to transfer Gag VLP production with the BEVS to bioreactor scale,[24] and advances made in the field provide an excellent opportunity to explore the production and quality of these nanoparticles.

In this work, the physicochemical properties and stability of HIV-1 VLPs produced in insect cells is initially addressed. Next, the quantity and quality of the Gag-eGFP VLPs produced in Hi5 and Sf9 cells, and its comparison to Gag VLP production is analyzed at nanoparticle level. Finally, aiming to establish an insect cell platform for the rapid production of Gag VLPs, a proof of concept in bioreactor is conducted.

MATERIALS AND METHODS

Insect cell lines and culture conditions

Hi5 cells (cat. no. B85502, Thermo Fisher Scientific, Grand Island, NY, USA) and Sf9 cells (cat. no. 71104, Merck, Darmstadt, Germany) were grown in the low-hydrolysate animal component-free Sf900III medium (Thermo Fisher Scientific). Hi5 and Sf9 cells were subcultured three times a week at a cell density of 2–4 $\times 10^5$ cells mL^{-1}[25] and 4–6 $\times 10^5$ cells mL^{-1}[26] in 125 mL disposable polycarbonate Erlenmeyer shake flasks (Corning, Steuben, NY, USA), respectively. All cultures were grown in an orbital shaker at 130 rpm (Stuart, Stone, UK) and maintained at 27 °C. Cell count and viability were measured with the Nucleocounter NC-3000 (Chemometec, Allerød, Denmark) using acridine orange for cell detection and 4′,6-diamidino-2-phenylindole (DAPI) (Chemometec) to quantify non-viable cells.

Recombinant BVs and infection conditions

The recombinant *Autographa californica* multicapsid nucleopolyhedrovirus (*Ac*MNPV) encoding a Rev-independent full-length HIV-1 *gag* gene fused in frame to eGFP (Gag-eGFP)[27] was constructed using the BaculoGold BV expression system (BD Biosciences, San Jose, CA, USA). The recombinant *Ac*MNPV encoding the full-length HIV-1 *gag* gene (GenBank accession no. K03455.1) codon-optimized for insect cell expression was developed with the Bac-to-Bac BV expression system (Thermo Fisher Scientific).[28] Both genes were under the control of the polyhedrin (polh) promoter.

Sf9 cells were used for BV amplification by infection at 3 $\times 10^6$ cells mL^{-1} and a multiplicity of infection (MOI) of 0.1. BV containing supernatants were harvested at 96 h post infection (hpi) at 1000 $\times g$ for 5 min. The number of infectious BV particles/mL was measured in Sf9 cells by the plaque assay method in 6-well plates (Nunc, Thermo Fisher Scientific).[22]

Production of Gag-eGFP and Gag VLPs in shake flasks

Hi5 and Sf9 cells were infected with BV-Gag or BV-Gag-eGFP in 125 mL Erlenmeyer shake flasks with 15 mL of Sf900III medium at conditions previously optimized. Briefly, exponentially growing Hi5 cells were infected with a MOI of 2.5 at 2 $\times 10^6$ cells mL^{-1}, and Gag or Gag-eGFP VLPs produced harvested at 69 hpi by centrifugation at 1000 $\times g$ for 5 min.[22] For Sf9 cells, BV infection was performed with a MOI of 0.01 at 3.7 $\times 10^6$ cells mL^{-1}, with VLPs harvested at 80 hpi.[23]

Production of Gag VLPs in bioreactor

A 2 L DASGIP® Bioblock glass bioreactor (Eppendorf, Hamburg, Germany) equipped with three Rushton impellers was used for Hi5 and Sf9 cell cultivation in 0.6 L working volume. Aeration was performed through a sparger to maintain the dissolved oxygen (DO) at 30% oxygen of air saturation. The air flow rate was set at 1 L h^{-1} and temperature at 27 °C. Initial agitation conditions were set at 150 rpm for Hi5 cells and 100 rpm for Sf9 cells. Agitation conditions were automatically adjusted in cascade control to aeration by the DASware control software (Eppendorf) to maintain the DO setpoint at 30% oxygen of air saturation. The pH was fixed at 6.4 for Hi5 cells and 6.2 for Sf9 cells and controlled with 20% *w/w* H_3PO_4 and 7.5% *w/w* $NaHCO_3$. Antifoam C (Sigma Aldrich, Saint Louis, MO, USA) was added to the cell culture by pulses to prevent foam formation.

Hi5 and Sf9 cells previously grown in 1 L Erlenmeyer shake flasks (Corning) were inoculated in the bioreactor at a final concentration of 1 $\times 10^6$ cells mL^{-1}. Hi5 and Sf9 cells were infected with BV-Gag at the same MOI used for shake flasks, when a viable cell concentration of 2 $\times 10^6$ and 3.7 $\times 10^6$ cell mL^{-1} was attained respectively. Gag-VLPs were harvested by centrifugation at 1000 $\times g$ for 5 min at the same conditions used in shake flasks.

Flow cytometry analysis of BV infection

The percentage of Gag-eGFP expressing cells was assessed using a BD FACS Canto II flow cytometer equipped with a 488 and 635 nm laser configuration (BD Biosciences, San Jose, CA, USA). For Gag expressing cells, a specific staining protocol was implemented. Shortly, cells were harvested at different times, washed, and fixed in 4% p-formaldehyde (Sigma) for 10 min at 4 °C. Afterwards, cells were washed and permeabilized using 0.1% (v/v) tween-20 (Sigma) for 15 min at room temperature (RT). Cells were washed again and blocked with 10% fetal bovine serum. After three washing cycles, cells were incubated with a rabbit anti-HIV-1 p24 primary antibody (EnoGene, New York, NY, USA) under mild rotation conditions for 1 h. Cells were then washed and incubated with a chicken anti-rabbit IgG secondary conjugated to Alexa Fluor 467 (Thermo Fisher Scientific) under continuous rotation for 2 h at RT in the dark. Cells were finally washed, resuspended in ice-cold phosphate buffered saline (PBS) solution and analyzed in the APC PMT detector of the flow

cytometer. A total of 2×10^4 cells were analyzed per sample at a flow rate of 10 µL min^{-1}. Single cells were gated according to side scatter (SSC-H) *versus* forward scatter (FSC-A) dot plots and Gag-eGFP (FITC-A) or Gag (APC-A) positive cells in comparison to a non-transfected control depending on their mean FITC-A or APC-A fluorescence intensity, respectively. Data acquisition and analysis was performed with the BD FACSDIVA software v.5.0 (BD Biosciences).

Gag-eGFP VLP characterization by ion exchange chromatography

An ÄKTA pure 25 M2 with an S9 sample pump and fraction collector F9-C (Cytiva, Marlborough, MA, USA) was used. Fifty milliliters and 43 mL of clarified cell culture supernatants containing Gag-eGFP VLPs produced in Hi5 and Sf9 cells, respectively, were filtered using a 0.8 µm Millex AA syringe filter (MilliporeSigma, Bedford, MA, USA) and loaded into 1 mL radial flow monolith column (CIMmultus™ QA, Sartorius, Göttingen, Germany).

Mobile phase A and B consisted in 50 mM HEPES, pH 7.2, and 50 mM HEPES, 2 M NaCl, pH 7.2, respectively. The column was equilibrated with 50 mM HEPES, 100 mM NaCl, pH 7.2 (5% v/v of buffer B) before loading. After column loading, a washing step with 15 column volumes (CV) of equilibration buffer (5% v/v of buffer B) was conducted. A 100–1000 mM NaCl (5–50% of buffer B) linear gradient at a flow rate of 1 mL min^{-1} was used to assess the VLP elution profile (50 CV). Samples were loaded into the column using the sample pump. Conductivity and ultraviolet (UV) absorbance at wavelengths of 280 and 260 nm were monitored using the software Unicorn (Cytiva).[29] Total protein concentration and double stranded DNA (dsDNA) quantification were conducted by the Bradford assay (BioRad Laboratories, Hercules, CA, USA) and QuantiTTM PicoGreen® dsDNA kit (Thermo Fisher Scientific) according to manufacturer's instructions.[29]

Nanoparticle quantification and characterization

Nanoparticle tracking analysis

VLP and total nanoparticle concentrations were measured by nanoparticle tracking analysis (NTA) using a NanoSight NS300 (Malvern Panalytical, Malvern, UK). Fluorescent particles measured were considered as VLPs, whereas all light-scattered particles were considered as total nanoparticles. Shortly, samples from harvested supernatants at 3000 × *g* for 5 min were diluted in 0.22 µm-filtered DPBS and continuously injected into the device chamber through a syringe pump at an average concentration of 10^8 particles mL^{-1} (20–60 particles $frame^{-1}$). Videos of 60 s from independent triplicate measurements were analyzed with the NanoSight NTA 3.2 software (Malvern Panalytical).

Flow virometry

VLP and total nanoparticle concentrations were assessed by flow cytometry using a CytoFlex LX (Beckman Coulter, Brea, CA, USA). Gating of the different populations was made according to SSC-A *versus* FITC-A dot plots and using fresh DPBS and Sf900III medium samples as negative controls. Samples from supernatants harvested at 3000 × *g* for 5 min were diluted in 0.22 µm-filtered DPBS and triplicate measurements from independent samples were analyzed with the CytExpert 2.3 software (Beckman Coulter).

Super-resolution fluorescence microscopy

The different nanoparticle populations in Gag and Gag-eGFP supernatants were analyzed with a TCS SP8 confocal microscope equipped with the Huygens deconvolution and LAS X software and GPU array (Leica Microsystems, Wetzlar, Germany) at Servei d'Anatomia Patològica from Hospital Sant Joan de Déu.[30] Briefly, nanoparticles were stained with 0.1% v/v of CellMask™ and 0.1% v/v of Hoechst 33342 or 0.05% v/v for Sf9-derived nanoparticles. Stained preparations were loaded onto a microscope slide and adsorbed to the surface of the cover glass (Linea LAB, Barcelona, Spain) for 30 min at RT. Analysis was conducted with 100× magnification (zoom 5) and a line average of 3 and 496 × 496 pixels with a HC PL APO CS2 100 X/1.40 OIL objective in the HyVolution2 mode (Leica). Five fields of 13 sections per each biological triplicate were analyzed. Deconvolution was performed with the SVI Huygens Professional program and the best resolution strategy (Scientific Volume Imaging B.V., Hilversum, the Netherlands). Particle size distribution (PSD) analyses were performed with the 3D module package in Imaris 8.2.1 (Bitplane, Oxford Instruments, Zurich, Switzerland) at Servei de Microscòpia from Institut de Neurociències (Universitat Autònoma de Barcelona).[20] PSD histograms were created with Microsoft Excel 2016 (Redmond, WA, USA).

Gag-eGFP quantification

The supernatants of insect cells infected with the BV-Gag-eGFP were recovered by centrifugation at 3000 × *g* for 5 min. Green fluorescence was measured with a Cary Eclipse fluorescence spectrophotometer (Agilent Technologies, Santa Clara, CA, USA) at RT as follows: $\lambda_{ex} = 488$ nm (5 nm slit), $\lambda_{em} = 500–530$ nm (10 nm slit). Relative fluorescence units were calculated by subtracting fluorescence unit values of fresh Sf900III medium.

Gag quantification

An HIV-1 p24 enzyme-linked immunosorbent assay (ELISA) kit (Sino Biological, Wayne, NJ, USA) was used to quantify the concentration of Gag polyprotein. Supernatants were harvested by centrifugation at 3000 × *g* for 5 min. Samples were incubated in SNCR buffer for 10 min at 70 °C, and in 1.5% Triton X-100 for 10 min at 100 °C. The substrate solution was prepared by dissolving a SIGMA*FAST* OPD substrate tablet and one urea hydrogen peroxide tablet (MilliporeSigma) at a final concentration of 0.4 mg mL^{-1} in deionized water. An HIV-1 p24 protein standard of known concentration was also included for absolute Gag quantification. The reaction was stopped by adding a 625 mM H_2SO_4 solution after 10 min incubation. The absorbance was measured at 492 nm with a reference wavelength at 630 nm in a Tecan Infinite 200 Pro reader (Tecan, Männedorf, Switzerland). p24 concentration values were corrected according to HIV-1 Gag molecular weight (55 kDa).

SDS-PAGE and western blot

Gag and Gag-eGFP VLP containing supernatants were examined by SDS-PAGE and western blot for HIV-1 p24 (A2-851-100, Icosagen, Tartu, Estonia) and GP64 (A2980, Abcam, Cambridge, UK) detection.[31]

Cryo-transmission electron microscopy

BV-Gag infected Sf9 and Hi5 cell supernatants at 80 and 69 hpi, respectively, were visualized with a cryo-transmission electron microscope. Two to three microliters of sample were blotted onto 400 mesh Holey carbon grids (Micro to Nano, Wateringweg, the Netherlands) previously subjected to glow discharge in a PELCO easiGlow discharge unit (Ted Pella Inc., Redding, CA, USA). Samples were subsequently plunged into liquid ethane at −180 °C

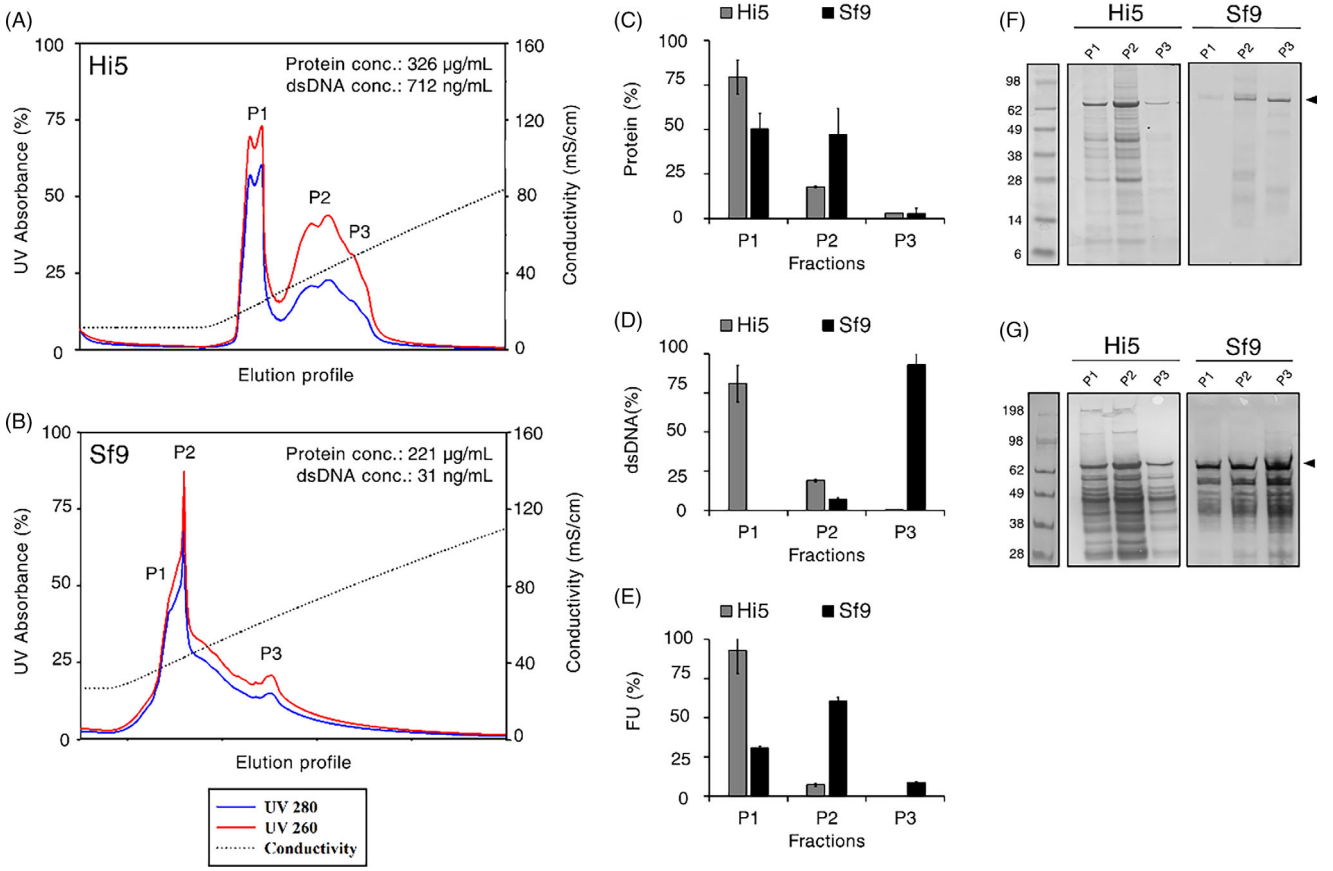

Figure 1. Characterization of Gag-eGFP VLPs produced in shake flasks. Elution profiles of infected Hi5 (A) and Sf9 cell (B) supernatants using a monolithic ion exchange column. The black dotted line in the chromatogram indicates conductivity, whereas blue and red lines refer to ultraviolate (UV) absorbance at 280 and 260 nm, respectively. Fluorescence (C), protein (D), and dsDNA distribution (E) in P1, P2, and P3 elution fractions. SDS-PAGE (F) and HIV-1 p24 western blot (G) analysis of P1, P2, and P3 elution fractions. The P1 fraction was diluted 1:2 before loading the SDS-PAGE and western blot. The black arrow corresponds to the band of the full-length Gag-eGFP polyprotein. Conc, concentration; FU, fluorescence units; dsDNA: double-stranded DNA.

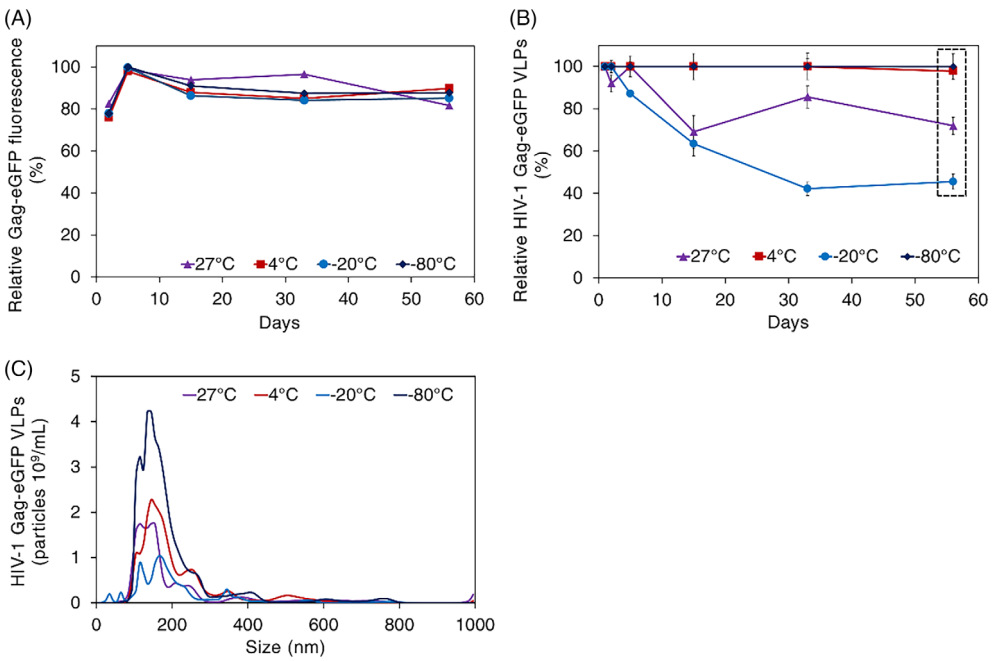

Figure 2. Stability profiles of Gag-eGFP VLPs in harvested supernatants stored at 27, 4, −20 and −80 °C. (A) Analysis of Gag-eGFP fluorescence by spectrofluorometry. (B) Analysis of VLP concentration by NTA. The first measurement in each condition was used as the reference to calculate relative percentages in subsequent readouts. (C) Size distribution of VLPs measured at day 56 post-freezing of the study [shown as a dashed square in Fig. 1(b)]. Fluorescent nanoparticles measured were considered as VLPs, whereas light-scattered particles were considered as total nanoparticles. NTA, nanoparticle tracking analysis; VLP, virus-like particle.

using a Leica EM GP cryo workstation (Leica) and observed in a Jeol JEM-2011 TEM electron microscope operating at 200 kV (Jeol Ltd., Akishima, Tokyo, Japan). During imaging, samples were maintained at −173 °C and pictures were taken using a CCD multiscan camera model no. 895 (Gatan Inc., Pleasanton, CA, USA).

Analysis of insect cell metabolism

Glucose, lactate, and phosphate concentrations were measured by ion-exclusion chromatography using a sulfonated polystyrene divinyl benzene column (Aminex HPX-87H, Bio-Rad, Hercules, CA, USA) in an Agilent 1200 series HPLC system (Agilent). A 0.01 N H_2SO_4 solution was used as the mobile phase with a flow rate of 0.45 mL min^{-1}. All measurements were performed in an AZURA UV/VIS detector (Knauer, Berlin, Germany) with a refractive index detector temperature of 35 °C. The standard deviation of the technique was determined as 0.31% for glucose, 0.26% for lactate, and 1.01% for phosphate measurement. The phosphate uptake rate was calculated taking into consideration the amount of phosphate present in the medium and also the volume of H_3PO_4 added for pH control.

Amino acid concentrations were determined by HPLC after derivatization in a reversed-phase Eclipse Plus C18 column (Agilent) at 40 °C according to manufacturer's instructions (Agilent). The flow rate was adjusted to 0.64 mL min^{-1} and two solvents (solution A and B) were used in the mobile phase. Solution A consisted of 10 mM K_2HPO_4 and 10 mM $K_2B_4O_7$, and solution B of a 45/45/10% *v/v/v* mix of acetonitrile, methanol and water, respectively. Amino acids were detected at 266/305 nm for fluorenylmethoxycarbonyl derivates and at 450 nm for o-phthalaldehyde derivates. The final amino acid concentration was quantified using an internal standard calibration. The standard deviation associated with the measurement of amino acid concentrations was 4 ± 1%.

RESULTS AND DISCUSSION

Physicochemical properties and quality assessment of HIV-1 VLPs

We have recently proven that the BV infection conditions of Hi5[22] and Sf9 cells[23] can be successfully optimized to produce high

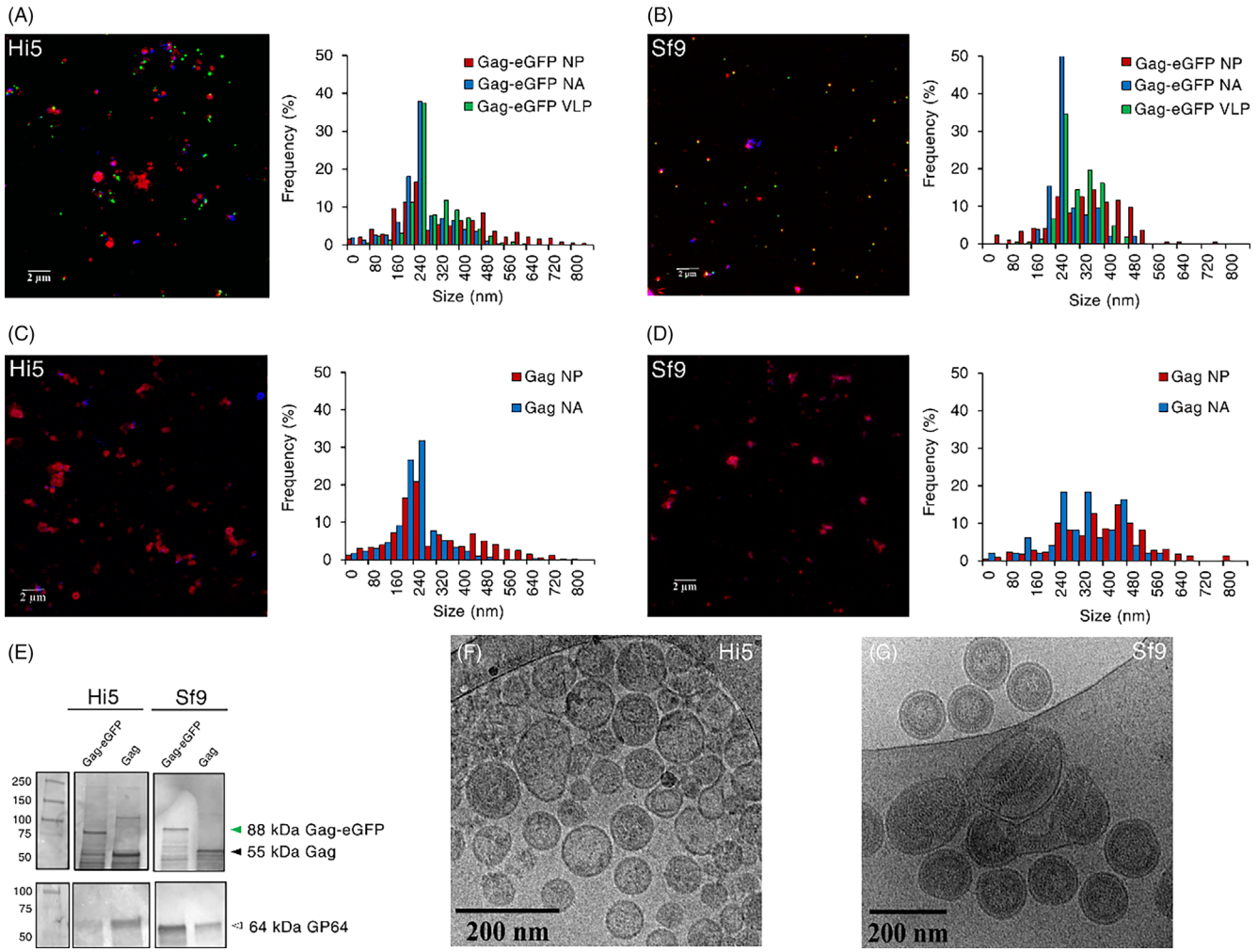

Figure 3. Analysis of Gag and Gag-eGFP VLPs. Imaging and assessment of size distribution by SRFM of the different nanoparticle populations in Hi5 (A) and Sf9 (B) supernatants infected with BV-Gag-eGFP. Nanoparticle lipid membranes were stained with CellMask™ (red) and nucleic acids with Hoechst (blue). Imaging and evaluation of size distribution by SRFM of the different nanoparticle populations in Hi5 (C) and Sf9 (D) supernatants infected with BV-Gag. (E) HIV-1 p24 (upper) and GP64 (lower) western blot analysis of Gag-eGFP and Gag VLP productions. The green mark indicates the Gag-eGFP band, the black mark shows the Gag band, and the white mark illustrates the GP64 band. Cryo-TEM micrographs of Gag VLPs produced in Hi5 (F) and Sf9 cells (G). NA, nucleic acid; NP, nanoparticle; SRFM, super-resolution fluorescence microscopy; VLP, virus-like particle.

Journal of Chemical Technology and Biotechnology published by John Wiley & Sons Ltd on behalf of Society of Chemical Industry (SCI).

HIV-1 VLP titers. However, the physicochemical properties and quality of these nanoparticles produced in both insect cell lines is still to be characterized. To this purpose, fluorescently tagged VLPs (Gag-eGFP VLPs) were used for an easier sample monitoring. Different parameters were assessed by ion exchange chromatography (IEX) in the unprocessed supernatant samples, including Gag-eGFP polyprotein (fluorescence units, FU), total protein concentration (μg mL^{-1}), and dsDNA concentration (ng mL^{-1}). A five-fold increase in FU was measured in Hi5 compared to Sf9 supernatants, with Sf9 supernatant samples exhibiting lower levels of contaminating protein and dsDNA (Fig. 1). The low Hi5 cell viability at harvest might explain the high amounts of dsDNA and proteins encountered in the supernatant. After IEX, there was no presence of VLPs in the flowthrough, supporting the complete capture of these nanoparticle by the monolith column (data not shown). Three different fractions, P1–P3, were pooled in each run according to UV 260 and 280 nm chromatograms. The three elution peaks were obtained at conductivities of 22, 38, and 51 mS cm^{-1} in the Hi5 supernatant [Fig. 1(A)], with similar conductivity values of 25, 31 and 51 mS cm^{-1} for P1–P3 in the Sf9 supernatant [Fig. 1(B)]. Most of the protein present in both Hi5 (80%) and Sf9 supernatants (50%) eluted at lower salt concentrations [Fig. 1(C)], whereas dsDNA eluted in P1 in the Hi5 and in P3 in the Sf9 supernatant, respectively [Fig. 1(D)]. The dsDNA elution profile of the Hi5 supernatant sample was comparable to that observed in Tnms42 cells,[32] while it was similar to the elution profile measured in CHO cells for the Sf9 supernatant.[33] Considering the different level of contaminants in each unpurified supernatant, as well as the strong positive charge of the quaternary amine monolithic column, a competition for binding between negative charged dsDNA and VLPs could be the reason behind the differences in dsDNA elution profiles.

The presence of Gag-eGFP VLPs was analyzed by spectrofluorometry (FU), SDS-PAGE, and HIV-1 p24 western blot in each pooled fraction [Fig. 1(E)–(G)]. The Gag-eGFP polyprotein was detected in all fractions analyzed, most of it eluting at a low conductivity in the Hi5 supernatant (93%), and at a low-intermediate salt concentration in the Sf9 supernatant (60%). Differences in the fluorescence elution pattern between cell lines could be attributed to the high ratio of unassembled Gag-eGFP monomer *versus* Gag-eGFP VLPs in the Hi5 supernatant,[22] since free monomer has been reported to elute earlier than VLPs.[29] Apart from the different content of unassembled Gag-eGFP monomer between both cells, similar HIV-1 VLP elution profiles in monolithic columns were observed in this work compared to other production platforms, with HIV-1 VLPs produced in HEK 293, Tnms42 and CHO cells eluting at conductivities of 27–49, ~20–45, and 45–90 mS cm^{-1}, respectively.[29,32,33]

Stability of HIV-1 VLPs

Product stability is an important parameter to consider towards extending the shelf-life of the product of interest. This is especially relevant when it comes to enveloped particulate products such as VLPs. To this purpose, the supernatant of VLPs produced with the BEVS was split, aliquoted, and maintained at four different conditions (27, 4, −20 and −80 °C) for 2 months. Gag-eGFP VLPs were used with the aim to discriminate VLPs from other nanoparticle populations co-expressed with the BEVS.[27] Different analytical techniques, including spectrofluorometry and NTA were employed (Fig. 2). VLP fluorescence was generally maintained over the 2-month period independently of the storage conditions used [Fig. 2(A)]. However, VLP characterization in native conditions by NTA revealed that the structural integrity of VLPs was only preserved at 4 and −80 °C [Fig. 2(B)], suggesting that VLPs stored at 27 and −20 °C were probably disassembling. Enhanced protease activity could explain the instability of VLPs stored at 27 °C, while particle disruption due to external and internal ice formation around the VLP envelope might explain the low stability at −20 °C.[34,35] Additionally, changes in the morphology were detected in all conditions except −80 °C [Fig. 2(C)]. So far, it is still not well known whether variations in VLP morphology can alter their immunogenicity profile. In any case, this data indicates that Gag VLPs produced with the BEVS can be safely stored at 4 and −80 °C for mid to long term purposes without the need of further purification.

Table 1. Quantification of Gag and Gag-eGFP VLP production titers and baculovirus particles in Hi5 and Sf9 cells infected with the BEVS in shake flasks. Nanoparticle quantification was performed by NTA and flow virometry, and i baculovirus particles were measured by the plaque assay method

Condition	Quantification method	Product	Fluorescent particles (10^9 particles mL^{-1})	Total particles (10^9 particles mL^{-1})
Hi5	NTA	Gag	n.a.	495 ± 60
		Gag-eGFP	34 ± 2	426 ± 61
	Flow virometry	Gag	n.a.	5.9 ± 0.5
		Gag-eGFP	2.2 ± 0.1	9.5 ± 0.3
Sf9	NTA	Gag	n.a.	128 ± 24
		Gag-eGFP	37 ± 9	181 ± 15
	Flow virometry	Gag	n.a.	5.9 ± 0.3
		Gag-eGFP	3.3 ± 0.3	8.2 ± 0.9
Sf900III medium	NTA	n.a.	n.a.	44.8 ± 1.9
	Flow virometry			0.1 ± 0.0

Condition	Product	IBV particles (10^7 pfu mL^{-1})
Hi5	Gag	10.0 ± 2.7
	Gag-eGFP	6.0 ± 1.4
Sf9	Gag	31.0 ± 13.5
	Gag-eGFP	76.7 ± 51.3

IBV, infectious baculovirus particle; n.a., not available.

Comparison of Gag-eGFP and Gag VLPs

Gag tagging with the fluorescent reporter protein eGFP is a useful strategy in bioprocess development since discrimination between other nanoparticle populations and VLPs is possible. This allows a better control and understanding of nanoparticle-based production platforms such as VLP expression with the BEVS. Nevertheless, once the bioprocess has been defined, the production of the final candidate without the fluorescent tag has to be assessed. Super-resolution fluorescence microscopy, a novel technique to characterize different nanoparticle populations simultaneously,[20] was applied to characterize Gag-eGFP and Gag VLP productions. Most of the Gag-eGFP VLPs produced in both insect cell lines were detected at the 150–250 nm range, as expected [Fig. 3(A) and (B)]. However, Sf9-derived Gag-eGFP VLPs proved to be more heterogeneous with a fraction of these VLPs with sizes in the 300–400 nm range. A higher number of nanoparticles was also measured at the 300–500 nm range in Sf9 supernatants. This could be related to the three to ten-fold higher concentration of BV particles in Sf9 over Hi5 supernatants (Table 1) given that these cells generally produce higher amounts of BVs. This is in agreement with the higher frequency of nucleic acid detection in the 300–500 nm range since BVs contain large genomes up to 180 kb.[36]

A similar size distribution was observed in Hi5 Gag VLP supernatants, with most of the nanoparticles located in the 150–250 nm size range [Fig. 3(C) and (D)]. Specific detection of Gag-eGFP and Gag in Hi5 and Sf9 supernatants was also confirmed by western blot, while the presence of the GP64 BV-associated protein also indicated the co-expression of BVs [Fig. 3(E)]. As Gag VLPs were not tagged, VLPs could not be differentiated from other nanoparticles, specifically extracellular vesicles (EVs), which fall in the same size range and have been described to be co-expressed with VLPs in animal cell lines.[30] These nanoparticles are generally produced at higher levels than VLPs, representing from 4 to 13-fold in Hi5 supernatants and from 2 to 5-fold in Sf9 supernatants,[26] with variability attributed to the quantification methodology employed

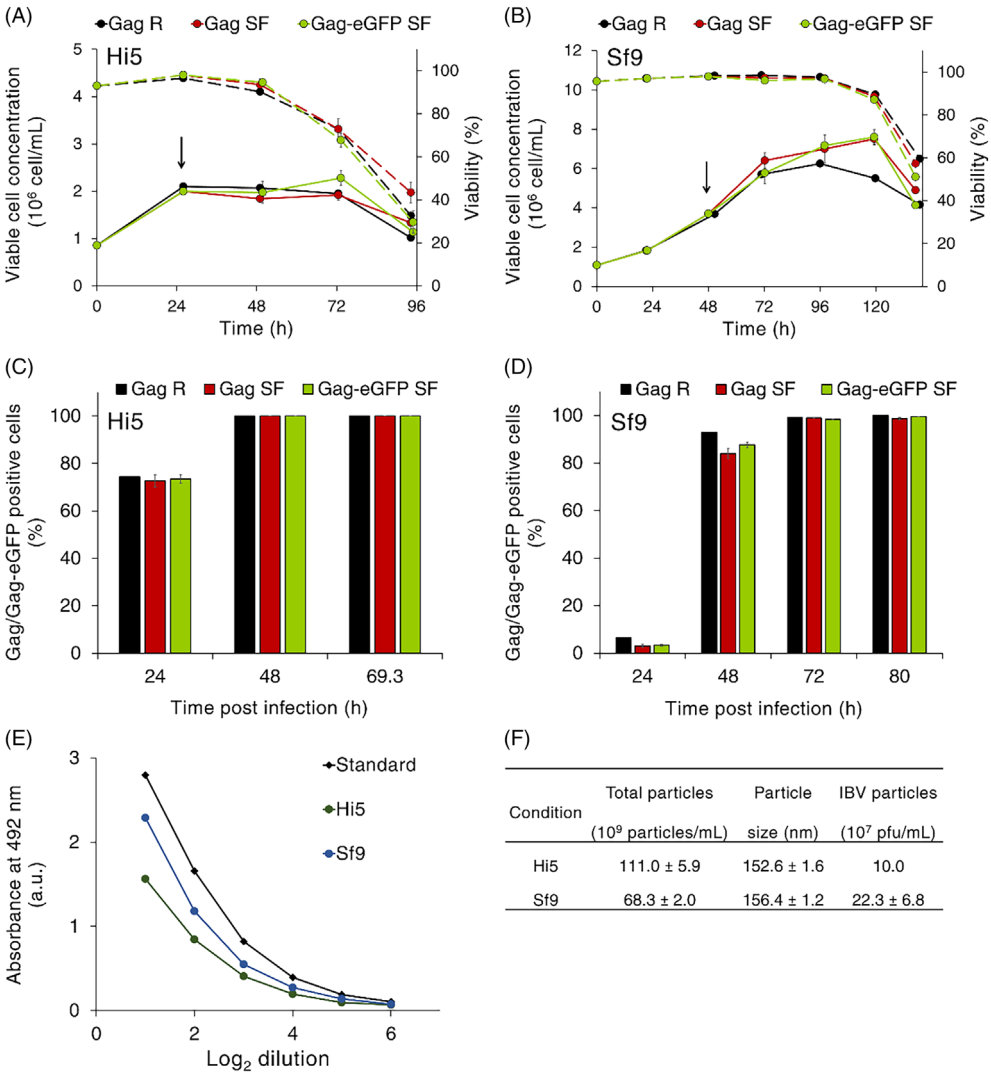

Condition	Total particles (10^9 particles/mL)	Particle size (nm)	IBV particles (10^7 pfu/mL)
Hi5	111.0 ± 5.9	152.6 ± 1.6	10.0
Sf9	68.3 ± 2.0	156.4 ± 1.2	22.3 ± 6.8

Figure 4. Transference of HIV-1 VLP production from shake flasks to bioreactor. Cell growth and viability profiles of Hi5 (A) and Sf9 cells (B). The black arrow indicates the time of recombinant baculovirus infection. Evolution of Gag and Gag-eGFP expression in Hi5 (C) and Sf9 cells (D) by flow cytometry after infection with recombinant baculoviruses. (E) Quantification of Gag production by enzyme-linked immunosorbent assay in the supernatant of infected insect cells cultured in bioreactor at the time of harvest. The HIV-1 p24 protein was included as standard of known concentration. (F) Measurement of total nanoparticles by NTA in the supernatant of infected insect cells cultured in bioreactor at the time of harvest. The concentration of infectious baculovirus particles in these conditions was also determined by the plaque assay method. IBV, infectious baculovirus; NTA, nanoparticle tracking analysis; R, bioreactor; SF, shake flask.

Journal of Chemical Technology and Biotechnology published by John Wiley & Sons Ltd on behalf of Society of Chemical Industry (SCI).

(Table 1). The higher load of BV particles in the Sf9 supernatant was also appreciated in Gag VLP preparations [Fig. 3(D)], with a larger nanoparticle population frequency in the 300–500 nm range compared to the Hi5 supernatant. Of note, it is possible that the concentration of BV particles was higher than the titers obtained by the plaque assay method due to the existence of defective BV particles.[37] The presence of nucleic acids in particles of similar sizes to VLPs was detected in Gag and Gag-eGFP preparations, possibly indicating that nanoparticles within this size range, VLPs, EVs or both, might contain or be associated with nucleotide molecules.[38,39] Further studies are needed to discriminate which nanoparticle populations are subjected to incorporate or associate to nucleic acids.

Gag VLP supernatants from both insect cell lines were analyzed by cryo-transmission electron microscopy (cryo-TEM). The native structure of Gag VLPs could be observed but differentiation of VLPs from EVs was more difficult in the Hi5 supernatant [Fig. 3(F) and (G)]. This is possibly due to the higher load of EVs co-expressed in Hi5 cells and also to the larger amounts of proteins (Fig. 2), which increase the background signal and reduce the quality of the imaging. Compared to previous studies with Gag-eGFP VLPs, Gag VLPs proved to be less heterogenous and with a higher degree of internal arrangement.[30] The absence of the eGFP fusion protein might result in the formation of more structured nanoparticles closely resembling immature HIV-1 virions.

Gag VLP production in bioreactor

The production of Gag VLPs with the insect cell/BEVS was assessed in a stirred tank bioreactor to test the feasibility of this platform for large scale VLP manufacture. Similar cell growth and infection kinetics were measured between shake flasks and bioreactors for Gag as well as Gag-eGFP production, indicating the successful transference of the conditions optimized in shake flasks to bioreactor scale [Fig. 4(A)–(D)]. The higher MOI used in Hi5 cells completely arrested cell growth after infection, whereas Sf9 cells continued to grow for the next 48 hpi. The same reason applies to the earlier decrease in cell viability and also the faster infection kinetics observed in Hi5 cells. After infection, an increase in stirring speed was observed in Hi5 cells, peaking at ~24 hpi, which could be related to a higher oxygen demand owing to the BV infection process since cell growth was completely arrested.[40] As for Sf9 cells, the maximum oxygen demand was recorded at ~40 hpi [Fig. 5 (A) and (B)], coinciding with the peak in viable cell concentration and complete infection. In these conditions, Hi5 and Sf9 cells yielded 1.86 and 1.28 mg L^{-1} of Gag polyprotein, with a higher amount of contaminant BV particles in the latter [Fig. 4(E) and (F)]. VLP titers in both platforms were higher than those achieved in insect cells by stable gene expression,[41-43] and transient transfection of plasmid DNA.[44,45] On the other hand, a larger load of contaminant EVs in the same size range as VLPs was observed in Hi5 cell cultures. Despite several advances to separate these contaminant species from Gag VLPs have been accomplished in the last years,[32,46] further research is still required. Moreover, it is not well known how these specimens might impact the final application of Gag VLPs, either by boosting their immunogenicity[47] or by reducing it.[48] If BV particles negatively impact the final application of Gag VLPs as a pharmaceutical product, Hi5 cells might be a better option for VLP production. If this is not the case, Sf9 cells might have an advantage since the presence of contaminating nucleic acids, host cell proteins and unassembled Gag, and EVs is lower, simplifying their purification. In any case, both platforms achieve superior Gag VLP yields in comparison to other systems employed to produce these nanoparticles at bioreactor scale,[49-51] and a three- to four-fold increase with respect to the most recent optimization study for Gag VLP production with the insect cell/BEVS.[52] Assuming a mouse is immunized with two doses of 5 μg of Gag VLPs in a prime-boost regimen[16] and not considering losses in process purification, a 1 L bioreactor culture of Sf9 or Hi5 cells would enable to immunize around 100–200 mice, respectively.

The analysis of cell metabolism is an important aspect to consider in bioprocess development since strategies for process intensification can be implemented. To this end, the metabolism of both insect cell lines cultured at bioreactor scale after BV infection was analyzed. Hi5 cells consumed larger levels of all the different

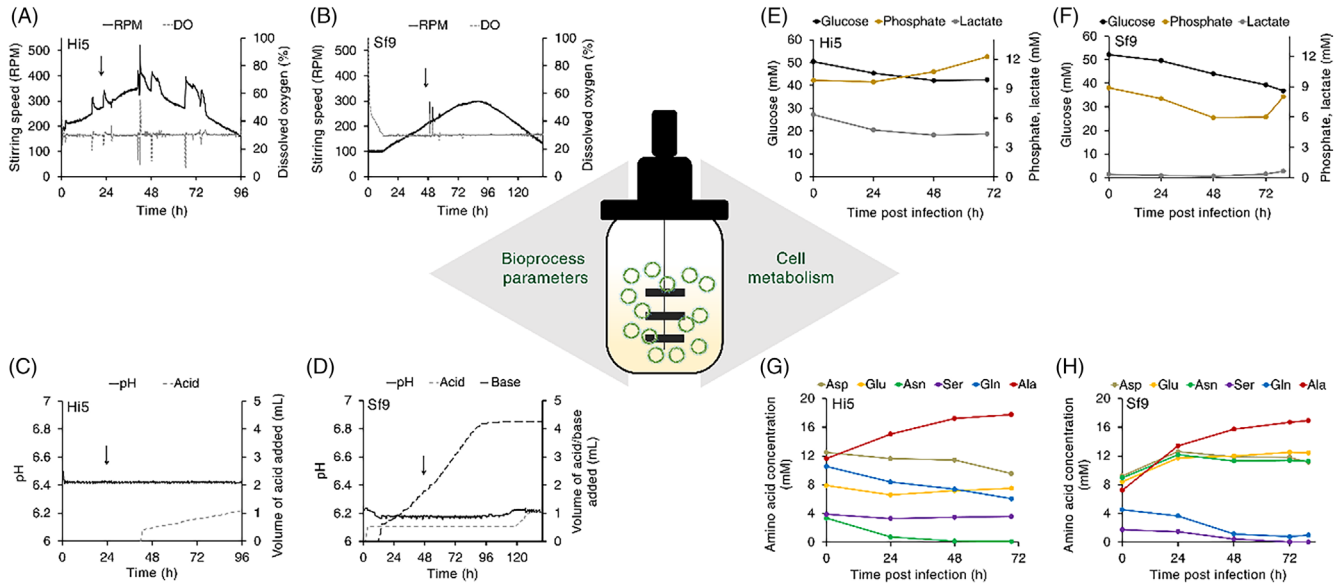

Figure 5. Analysis of bioreactor parameters with the insect cell/BEVS. Stirring speed, dissolved oxygen concentration, pH, and volume of acid/base added in Hi5 (A,C) and Sf9 cell (B,D) cultures. Black arrows indicate the time point of recombinant baculovirus infection. Profiles of glucose, lactate, phosphate (E,F) and main amino acids produced/consumed (G,H) in Hi5 and Sf9 cultures, respectively. Ala, alanine; Asn, asparagine; Asp, aspartic acid; DO, dissolved oxygen; Gln, glutamine; Glu, glutamic acid; RPM, revolutions per minute; Ser, serine.

metabolites assessed in comparison to Sf9 cells [Fig. 5(E)–(H)], with glucose, asparagine, and glutamine as the most highly consumed (Supporting Information, Fig. S1). Asparagine is reported as the principal nitrogen source for Hi5 cells and its uptake rate can be even higher than glucose.[53] After BV infection, asparagine was not consumed as rapid as previously observed,[41] possibly due to the low concentration in the medium at the time of infection, resulting in complete asparagine exhaustion between 24–48 hpi and coinciding with the decline in cell viability. Sf9 cells exhibited a more balanced metabolism with reduced uptake fluxes of the different metabolites analyzed (Supporting Information, Fig. S1). Glucose, the principal carbon source, and glutamine, an important nitrogen source in insect cell cultures, were the main compounds consumed by Sf9 cells. None of them was limiting by the end of the production phase, though the low concentration of glutamine in the medium (~1 mM) could have possibly influenced its uptake by Sf9 cells. Interestingly, serine was depleted at 48 hpi, coinciding with the peak of maximum viable cell concentration and complete BV infection. Thus, asparagine and serine supplementation at the time of infection could be an option to extend the productive time of Hi5 and Sf9 cells, respectively, and further increase VLP yields.

The control of bioprocess parameters in the bioreactor was successfully achieved in both insect cell lines. However, differences in the behavior of Hi5 and Sf9 cells were observed [Fig. 5(C) and (D)]. The addition of sodium bicarbonate to the Sf9 cell culture by the software control loop at the beginning of the bioreactor operation indicated the acidification of the culture medium. The accumulation of organic acids derived from cell metabolism such as glutamic and aspartic acid, both with pKa values below the cell culture pH, and CO_2 production from cell respiration could be the reasons behind medium acidification. On the contrary, the addition of phosphoric acid to the Hi5 cell culture was detected. Ammonia formation, a by-product of insect cell metabolism, could explain medium basification since significantly higher asparagine and glutamine uptake rates were measured in this cell line.[54] Alanine was also produced in both bioreactor cultures peaking in the 15–20 mM range. The formation of this amino acid is a feature observed in animal cell metabolism under glucose excess conditions.[55] Lactate, another by-product of insect cell metabolism, was not produced after BV infection, which is probably associated to pH and dissolved oxygen concentration maintenance along the culture.[56]

CONCLUSIONS

This study provides a detailed analysis of the insect cell/BEVS and shows the versatility of this system to produce HIV-1 VLPs. VLPs produced in the reference Hi5 and Sf9 insect cell lines exhibit similar physicochemical properties and are stable when stored at −80 °C for 2 months with little impact on their morphology. Gag VLP titers are similar to those obtained for Gag-eGFP VLPs, with nanoparticle sizes in the 150–250 nm range closely resembling immature HIV-1 virions. A high degree of heterogeneity and complexity is detected in VLP productions, with large concentrations of EVs, dsDNA and total protein content in Hi5 supernatants, whereas high loads of BV particles are encountered in Sf9 supernatants. The successful transference of Gag VLP production from shake flasks to stirred tank bioreactor is demonstrated, providing two different strategies to produce these complex nanoparticles in large volumes with controlled operational conditions.

ACKNOWLEDGEMENTS

The authors thank Alois Jungbauer (University of Natural Resources and Life Sciences, Vienna, Austria) for facilitating the access to ÄKTA pure system, and Paula Alves (Instituto de Biologia Experimental e Tecnológica, Oeiras, Portugal) for providing the Hi5 cell line. We also appreciate the support of Miriam Klausberger on the protocol for Gag staining, Krisztina Koczka for providing the BV-Gag stock, Sahar Masoumeh Ghorbanpour with ELISA quantification, Martí de Cabo (Servei de Microscòpia, Universitat Autònoma de Barcelona) with cryo-TEM, Mónica Roldán (Unitat de Microscòpia Confocal, Servei d'anatomia Patològica, Institut Pediàtric de Malalties Rares, Hospital Sant Joan de Déu) with SRFM, and Jorge Fomaro and Ángel Calvache (Beckman Coulter) for facilitating the access to the CytoFlex LX. Eduard Puente-Massaguer (FPU15/03577) and Irene González-Domínguez (FPU16/02555) are recipients of FPU grants from Ministerio de Educación, Cultura y Deporte of Spain. The research group is recognized as 2017 SGR 898 by Generalitat de Catalunya.

SUPPORTING INFORMATION

Supporting information may be found in the online version of this article.

REFERENCES

1 Stolt-Bergner P, Benda C, Bergbrede T, Besir H, Celie PHN, Chang C *et al.*, Baculovirus-driven protein expression in insect cells: a benchmarking study. *J Struct Biol* **203**:71–80 (2018).
2 Contreras-Gómez A, Sánchez-Mirón A, García-Camacho F, Molina-Grima E and Chisti Y, Protein production using the baculovirus-insect cell expression system. *Biotechnol Prog* **30**:1–18 (2014).
3 Weber W and Fussenegger M, *Insect Cell-Based Recombinant Protein Production*. Springer Heidelberg, Berlin, pp. 263–277 (2009).
4 Merten OW and Gaillet B, Viral vectors for gene therapy and gene modification approaches. *Biochem Eng J* **108**:98–115 (2016).
5 Dai X, Jian C, Na L, Wang X, Dai Y and Li D, Production and characterization of Hantaan virus-like particles from baculovirus expression system. *Biochem Eng J* **152**:107373 (2019).
6 Ding X, Liu D, Booth G, Gao W and Lu Y, Virus-like particle engineering: from rational design to versatile applications. *Biotechnol J* **13**:1–7 (2018).
7 Zepeda-Cervantes J, Ramírez-Jarquín JO and Vaca L, Interaction between virus-like particles (VLPs) and pattern recognition receptors (PRRs) from dendritic cells (DCs): toward better engineering of VLPs. *Front Immunol* **11**:1100 (2020).
8 Nooraei S, Bahrulolum H, Hoseini ZS, Katalani C, Hajizade A, Easton AJ *et al.*, Virus-like particles: preparation, immunogenicity and their roles as nanovaccines and drug nanocarriers. *J Nanobiotechnol* **19**:59 (2021).
9 Biddlecome A, Habte HH, McGrath KM, Sambanthamoorthy S, Wurm M, Sykora MM *et al.*, Delivery of self-amplifying RNA vaccines in in vitro reconstituted virus-like particles. *PLoS One* **14**:e0215031 (2019).
10 Prel A, Caval V, Gayon R, Ravassard P, Duthoit C, Payen E *et al.*, Highly efficient in vitro and in vivo delivery of functional RNAs using new versatile MS2-chimeric retrovirus-like particles. *Mol Ther Methods Clin Dev* **2**:15039 (2015).
11 Finbloom J, Aanei I, Bernard J, Klass S, Elledge S, Han K *et al.*, Evaluation of three morphologically distinct virus-like particles as nanocarriers for convection-enhanced drug delivery to glioblastoma. *Nanomaterials.* **8**:1007 (2018).
12 Peyret H, Gehin A, Thuenemann EC, Blond D, El Turabi A, Beales L *et al.*, Tandem fusion of hepatitis B core antigen allows assembly of virus-like particles in bacteria and plants with enhanced capacity to accommodate foreign proteins. *PLoS One.* **10**:e0120751 (2015).
13 Enomoto T, Kawano M, Fukuda H, Sawada W, Inoue T, Haw KC *et al.*, Viral protein-coating of magnetic nanoparticles using simian virus 40 VP1. *J Biotechnol* **167**:8–15 (2013).
14 Theillet G, Martinez J, Steinbrugger C, Lavillette D, Coutard B, Papageorgiou N *et al.*, Comparative study of chikungunya virus-like particles and pseudotyped-particles used for serological detection

Journal of Chemical Technology and Biotechnology published by John Wiley & Sons Ltd on behalf of Society of Chemical Industry (SCI).

of specific immunoglobulin M. *Virology* **529**:195–204 (2019). https://doi.org/10.1016/j.virol.2019.01.027.
15 Fontana D, Garay E, Cevera L, Kratje R, Prieto C and Gòdia F, Chimeric vlps based on hiv-1 gag and a fusion rabies glycoprotein induce specific antibodies against rabies and foot-and-mouth disease virus. *Vaccine* **9**:251 (2021).
16 Nika L, Cuadrado-Castano S, Arunkumar GA, Grünwald-Gruber C, McMahon M, Koczka K *et al*., An HER2-displaying virus-like particle vaccine protects from challenge with mammary carcinoma cells in a mouse model. *Vaccine* **7**:1–19 (2019).
17 Kaczmarczyk SJ, Sitaraman K, Young HA, Hughes SH and Chatterjee DK, Protein delivery using engineered virus-like particles. *Proc Natl Acad Sci U S A* **108**:16998–17003 (2011).
18 Lavado-García J, Jorge I, Boix-Besora A, Vázquez J, Gòdia F and Cervera L, Characterization of HIV-1 virus-like particles and determination of gag stoichiometry for different production platforms. *Biotechnol Bioeng* **118**:2660–2675 (2021).
19 Alvim RGF, Itabaiana I and Castilho LR, Zika virus-like particles (VLPs): stable cell lines and continuous perfusion processes as a new potential vaccine manufacturing platform. *Vaccine* **37**:6970–6977 (2019).
20 González-Domínguez I, Puente-Massaguer E, Cervera L and Gòdia F, Quantification of the HIV-1 virus-like particle production process by super-resolution imaging: from VLP budding to nanoparticle analysis. *Biotechnol Bioeng* **117**:1929–1945 (2020).
21 Puente-Massaguer E, Cajamarca-Berrezueta B, Volart A, González-Domínguez I and Gòdia F, Transduction of HEK293 cells with BacMam baculovirus is an efficient system for the production of HIV-1 virus-like particles. *Viruses* **14**:636 (2022).
22 Puente-Massaguer E, Lecina M and Gòdia F, Integrating nanoparticle quantification and statistical design of experiments for efficient HIV-1 virus-like particle production in high five cells. *Appl Microbiol Biotechnol* **104**:1569–1582 (2020).
23 Puente-Massaguer E, Lecina M and Gòdia F, Application of advanced quantification techniques in nanoparticle-based vaccine development with the Sf9 cell baculovirus expression system. *Vaccine* **38**:1849–1859 (2020).
24 Cruz PE, Cunha A, Peixoto CC, Clemente J, Moreira JL and Carrondo MJT, Optimization of the production of virus-like particles in insect cells. *Biotechnol Bioeng* **60**:408–418 (1998).
25 Puente-Massaguer E, Lecina M and Gòdia F, Nanoscale characterization coupled to multi-parametric optimization of Hi5 cell transient gene expression. *Appl Microbiol Biotechnol* **102**:10495–10510 (2018).
26 Puente-Massaguer E, Saccardo P, Ferrer-Miralles N, Lecina M and Gòdia F, Coupling microscopy and flow cytometry for a comprehensive characterization of nanoparticle production in insect cells. *Cytometry A* **97**:921–932 (2020).
27 Hermida-Matsumoto L and Resh MD, Localization of human immunodeficiency virus type 1 Gag and Env at the plasma membrane by confocal imaging. *J Virol* **74**:8670–8679 (2000).
28 Nika L, Wallner J, Palmberger D, Koczka K, Vorauer-Uhl K and Grabherr R, Expression of full-length HER2 protein in Sf9 insect cells and its presentation on the surface of budded virus-like particles. *Protein Expr Purif* **136**:27–38 (2017).
29 Pereira Aguilar P, González-Domínguez I, Schneider TA, Gòdia F, Cervera L and Jungbauer A, At-line multi-angle light scattering detector for faster process development in enveloped virus-like particle purification. *J Sep Sci* **42**:2640–2649 (2019).
30 González-Domínguez I, Puente-Massaguer E, Cervera L and Gòdia F, Quality assessment of virus-like particles at single particle level: a comparative study. *Viruses* **12**:223–235 (2020).
31 Steppert P, Burgstaller D, Klausberger M, Kramberger P, Tover A, Berger E *et al*., Separation of HIV-1 gag virus-like particles from vesicular particles impurities by hydroxyl-functionalized monoliths. *J Sep Sci* **40**:979–990 (2017).
32 Reiter K, Aguilar PP, Grammelhofer D, Joseph J, Steppert P and Jungbauer A, Separation of influenza virus-like particles from baculovirus by polymer grafted anion-exchanger. *J. Sep. Sci* **43**:2270-2278 (2020).
33 Steppert P, Burgstaller D, Klausberger M, Berger E, Aguilar PP, Schneider TA *et al*., Purification of HIV-1 gag virus-like particles and separation of other extracellular particles. *J Chromatogr A* **1455**:93–101 (2016).
34 Lynch A, Meyers AE, Williamson A-LL and Rybicki EP, Stability studies of HIV-1 Pr55gag virus-like particles made in insect cells after storage in various formulation media. *Virol J* **9**:210 (2012).
35 González-Domínguez I, Lorenzo E, Bernier A, Cervera L, Gòdia F and Kamen A, A four-step purification process for gag vlps: from culture supernatant to high-purity lyophilized particles. *Vaccine* **9**:1154 (2021).
36 van Oers M and Vlak J, Baculovirus genomics. *Curr Drug Targets* **8**:1051–1068 (2007).
37 Wickham TJ, Davis T, Granados RR, Hammer DA, Shuler ML and Wood HA, Baculovirus defective interfering particles are responsible for variations in recombinant protein production as a function of multiplicity of infection. *Biotechnol Lett* **13**:483–488 (1991).
38 Valley-Omar Z, Meyers AE, Shephard EG, Williamson A-L and Rybicki EP, Abrogation of contaminating RNA activity in HIV-1 gag VLPs. *Virol J* **8**:462 (2011).
39 Fatima F and Nawaz M, Vesiculated long non-coding RNAs: offshore packages deciphering trans-regulation between cells, cancer progression and resistance to therapies. *Noncoding RNA* **3**:10 (2017).
40 Lecina M, Soley A, Gràcia J, Espunya E, Lázaro B, Cairó JJ *et al*., Application of on-line OUR measurements to detect actions points to improve baculovirus-insect cell cultures in bioreactors. *J Biotechnol* **125**:385–394 (2006).
41 Puente-Massaguer E, Grau-Garcia P, Strobl F, Grabherr R, Striedner G, Lecina M *et al*., Accelerating HIV-1 VLP production using stable high five insect cell pools. *Biotechnol J* **16**:1–12 (2021).
42 Puente-Massaguer E, Grau-Garcia P, Strobl F, Grabherr R, Striedner G, Lecina M *et al*., Stable Sf9 cell pools as a system for rapid HIV-1 virus-like particle production. *J Chem Technol Biotechnol* **96**:3388–3397 (2021).
43 Vidigal J, Fernandes B, Dias MM, Patrone M, Roldão A, Carrondo MJT *et al*., RMCE-based insect cell platform to produce membrane proteins captured on HIV-1 gag virus-like particles. *Appl Microbiol Biotechnol* **102**:655–666 (2018).
44 Puente-Massaguer E, Gòdia F and Lecina M, Development of a non-viral platform for rapid virus-like particle production in Sf9 cells. *J Biotechnol* **322**:43–53 (2020).
45 Puente-Massaguer E, Strobl F, Grabherr R, Striedner G, Lecina M and Gòdia F, PEI-mediated transient transfection of high five cells at bioreactor scale for HIV-1 VLP production. *Nanomaterials* **10**:1–16 (2020).
46 Reiter K, Aguilar PP, Wetter V, Steppert P, Tover A and Jungbauer A, Separation of virus-like particles and extracellular vesicles by flow-through and heparin affinity chromatography. *J Chromatogr A* **1588**:77–84 (2019).
47 Heinimäki S, Tamminen K, Malm M, Vesikari T and Blazevic V, Live baculovirus acts as a strong B and T cell adjuvant for monomeric and oligomeric protein antigens. *Virology* **511**:114–122 (2017).
48 Thompson CM, Petiot E, Mullick A, Aucoin MG, Henry O and Kamen A, Critical assessment of influenza VLP production in Sf9 and HEK293 expression systems. *BMC Biotechnol* **15**:1–12 (2015).
49 Sakuragi S, Goto T, Sano K and Morikawa Y, HIV type 1 Gag virus-like particle budding from spheroplasts of saccharomyces cerevisiae. *Proc Natl Acad Sci U S A* **99**:7956–7961 (2002).
50 Fernandes B, Vidigal J, Correia R, Carrondo MJT, Alves PM, Teixeira AP *et al*., Adaptive laboratory evolution of stable insect cell lines for improved HIV-Gag VLPs production. *J Biotechnol* **307**:139–147 (2020).
51 Fernandes B, Correia R, Sousa M, Carrondo MJT, Alves PM and Roldão A, Integrating high cell density cultures with adapted laboratory evolution for improved Gag-HA virus-like particles production in stable insect cell lines. *Biotechnol Bioeng* **118**:2536–2547 (2021).
52 Pillay S, Meyers A, Williamson AL and Rybicki EP, Optimization of chimeric HIV-1 virus-like particle production in a baculovirus-insect cell expression system. *Biotechnol Prog* **25**:1153–1160 (2009).
53 Monteiro F, Bernal V and Alves PM, The role of host cell physiology in the productivity of the baculovirus-insect cell system: fluxome analysis of Trichoplusia ni and Spodoptera frugiperda cell lines. *Biotechnol Bioeng* **114**:674–684 (2017).
54 Rhiel M, Mitchell-Logean CM and Murhammer DW, Comparison of Trichoplusia ni BTI-Tn-5b1-4 (high five) and Spodoptera frugiperda Sf-9 insect cell line metabolism in suspension cultures. *Biotechnol Bioeng* **55**:909–920 (1997).
55 Benslimane C, Elias CB, Hawari J and Kamen A, Insights into the central metabolism of Spodoptera frugiperda (Sf-9) and Trichoplusia ni BTI-Tn-5B1-4 (Tn-5) insect cells by radiolabeling studies. *Biotechnol Prog* **21**:78–86 (2005).
56 Strobl F, Ghorbanpour SM, Palmberger D and Striedner G, Evaluation of screening platforms for virus-like particle production with the baculovirus expression vector system in insect cells. *Sci Rep* **10**:1065 (2020).